Supplementary Information

Realizing Superior Prussian Blue Positive Electrode for Potassium Storage via Ultrathin Nanosheet Assembly

Mingsheng Qin,[†] Wenhao Ren,[‡] Jiashen Meng,[†] Xuanpeng Wang,[†] Xuhui Yao,[†] Yajie Ke,[†] Qi Li*[†] and Liqiang Mai[†]

[†]State Key Laboratory of Advanced Technology for Materials Synthesis and Processing, Wuhan University of Technology, Wuhan 430070, Hubei, China.

[‡]School of Chemistry, Faculty of Science, The University of New South Wales, Sydney, New South Wales 2052, Australia.

*Corresponding Author

E-mail: qi.li@whut.edu.cn

Number of Pages: 11 (S1-S11)

Number of Figures: 17 (Fig. S1-S17)

Number of Tables: 1 (Table S1)

Content

Fig S1. SEM image of PB-NBs.

Fig S2. SEM and TEM images of PB-NSs.

Fig S3. X-ray photoelectron spectroscopy (XPS) results for PB-NSs.

Fig S4. Elements distribution of PB-NSs.

Fig S5. Thermogravimetric analysis of PB-NSs and PB-NBs.

Fig S6. FT-IR spectra for PB-NSs and PB-NBs.

Fig S7. CV curves at a scan rate of 0.1 mV s^{-1} for (a) PB-NSs and (b) PB-NBs.

Fig S8. The first charge-discharge curves of PB-NSs and PB-NBs at a current density of 50 mA g^{-1}.

Fig S9. The third charge-discharge curves of PB-NSs and PB-NBs at a current density of 50 mA g^{-1}.

Fig S10. The charge-discharge curves of (a) PB-NSs and (b) PB-NBs at different rates.

Fig S11. The cycling performance of PB-NSs at 50 mA g^{-1}.

Fig S12. The SEM image for (a) PB-NSs and (b) PB-NBs after 100 cycles at 50 mA g^{-1}.

Fig S13. XRD patterns of pristine and cycled electrode materials for (a) PB-NSs and (b) PB-NBs.

Fig S14. The (a) HRTEM image and (c) SAED pattern of pristine PB-NSs. (b) HRTEM image and (d) SAED pattern of PB-NSs after 20 cycles at 50 mA g^{-1}.

Fig S15. The regional GITT potential response curves with time.

Fig S16. The Schematic of ions and charge transport process.

Fig S17. Raman spectra collected at different charge and discharge states for PB-NSs at 50 mA g^{-1}.

Table S1. ICP results of the PB-NSs and PB-NBs

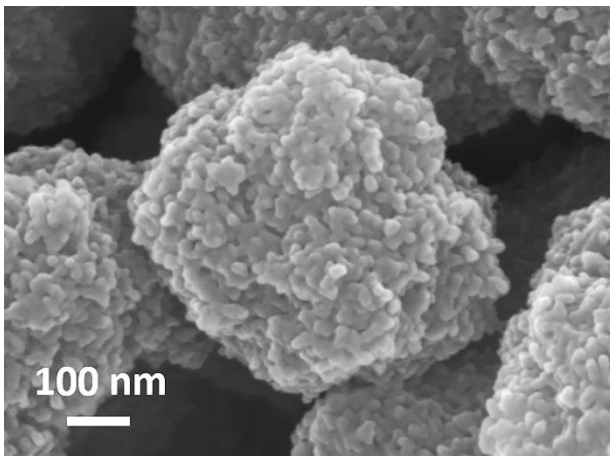

Fig S1. SEM image of PB-NBs.

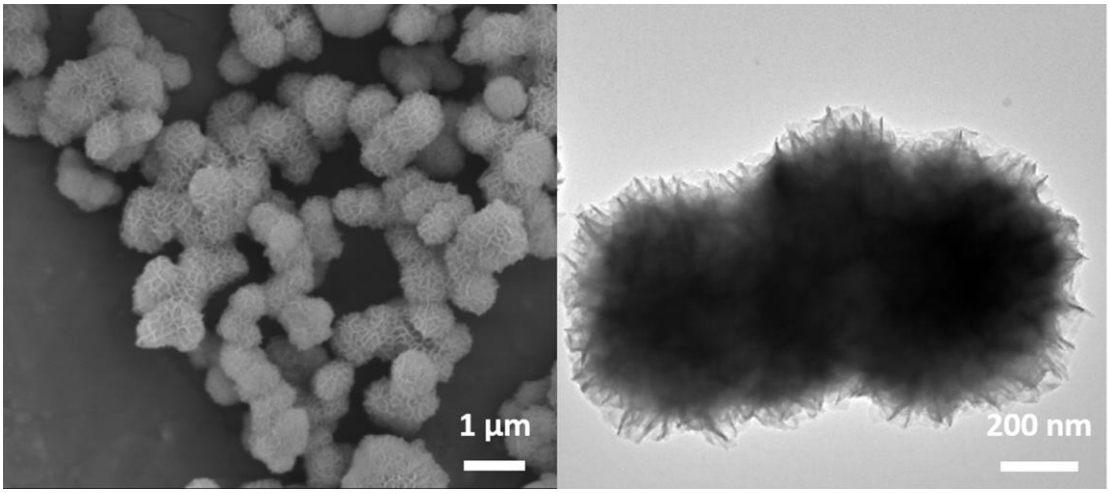

Fig S2. SEM and TEM images of PB-NSs.

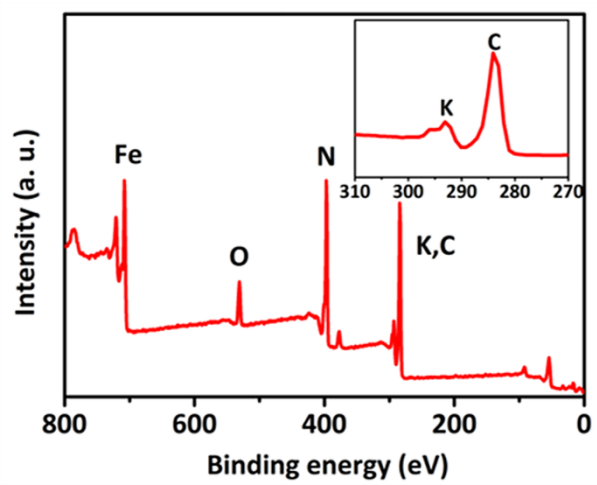

Fig S3. X-ray photoelectron spectroscopy (XPS) results for PB-NSs.

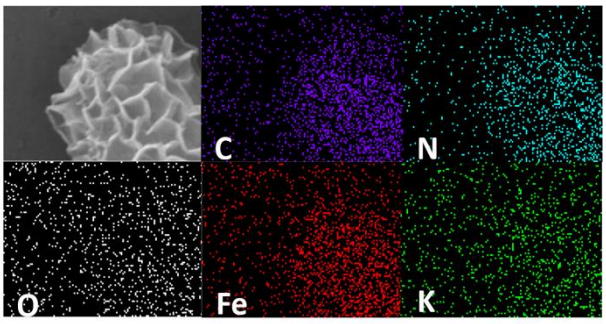

Fig S4. Elements distribution of PB-NSs.

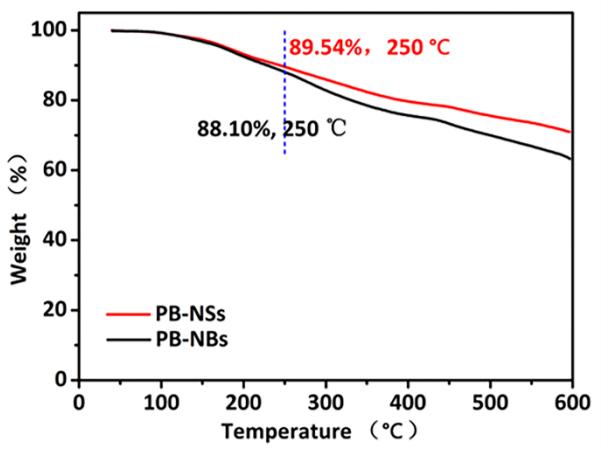

Fig S5. Thermogravimetric analysis of PB-NSs and PB-NBs.

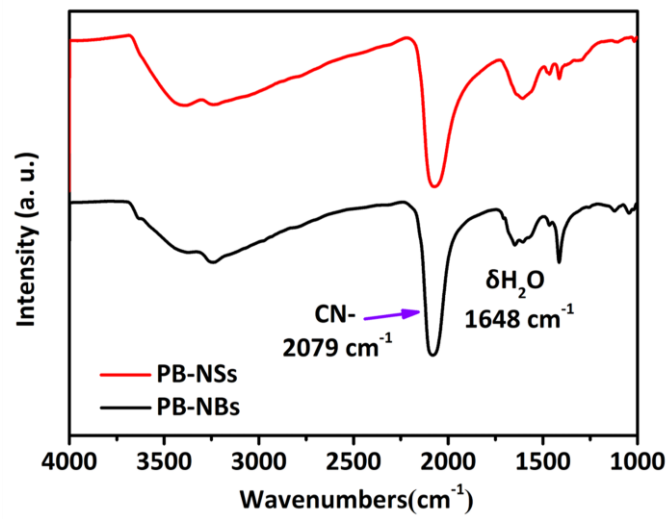

Fig S6. FT-IR spectra for PB-NSs and PB-NBs.

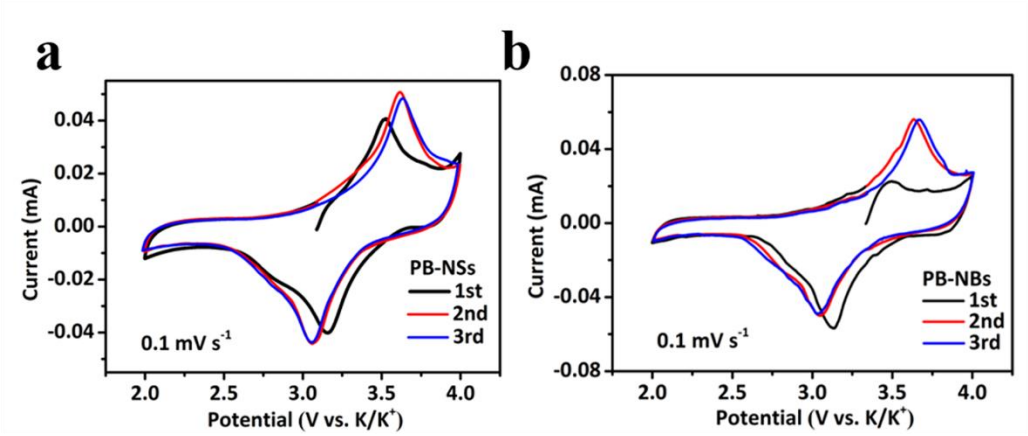

Fig S7. CV curves at a scan rate of 0.1 mV s^{-1} for (a) PB-NSs and (b) PB-NBs.

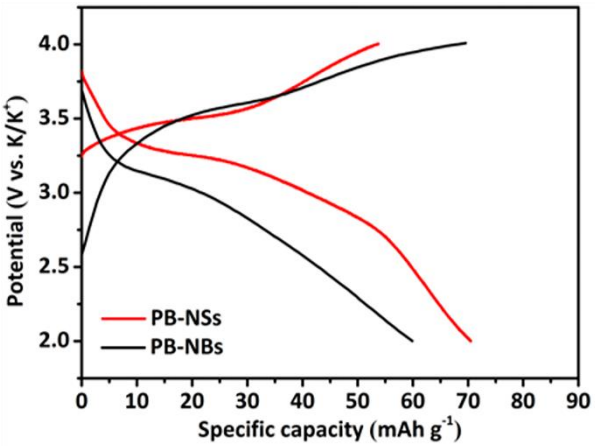

Fig S8. The first charge-discharge curves of PB-NSs and PB-NBs at a current density of 50 mA g^{-1}.

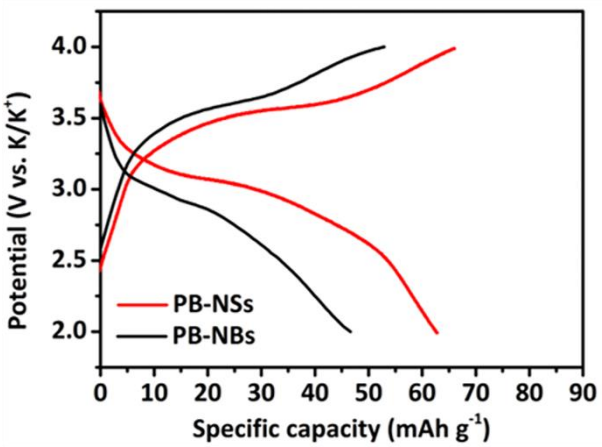

Fig S9. The third charge-discharge curves of PB-NSs and PB-NBs at a current sensity of 50 mA g^{-1}.

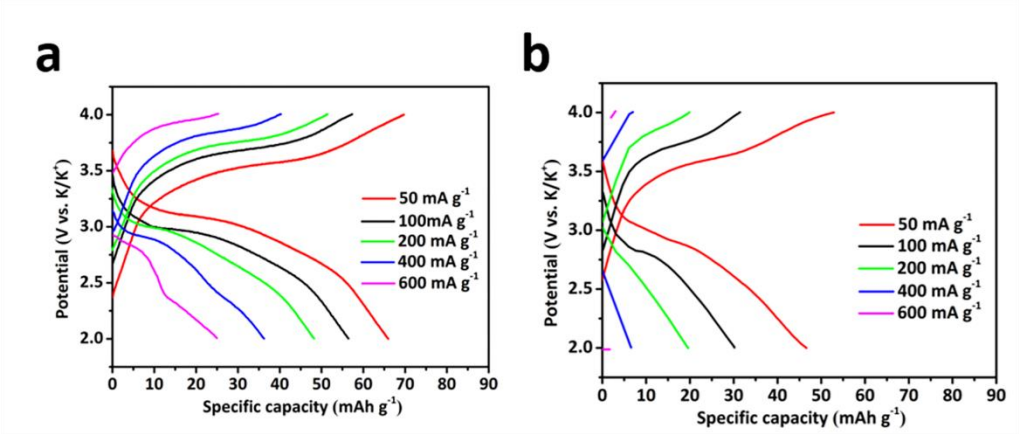

Fig S10. The charge-discharge curves of (a) PB-NSs and (b) PB-NBs at different rates.

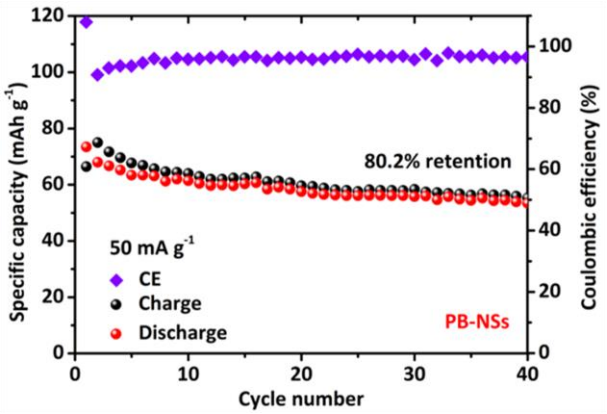

Fig S11. The cycling performance of PB-NSs at 50 mA g^{-1}.

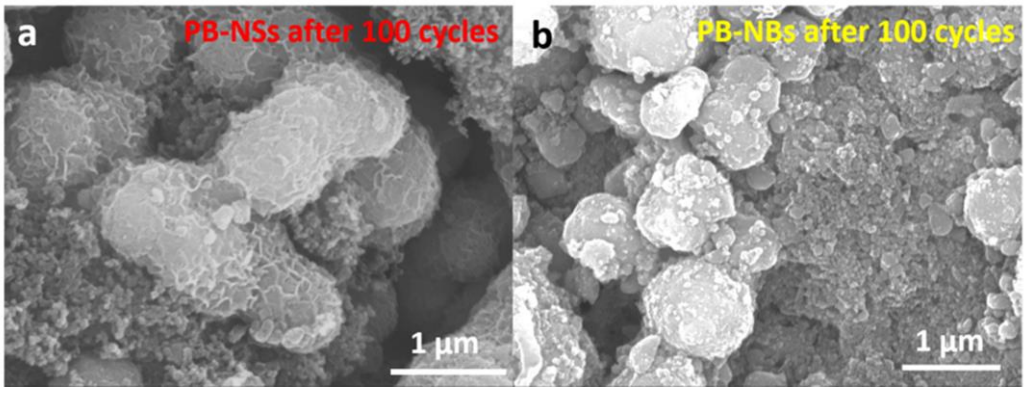

Fig S12. The SEM image for (a) PB-NSs and (b) PB-NBs after 100 cycles at 50 mA g^{-1}.

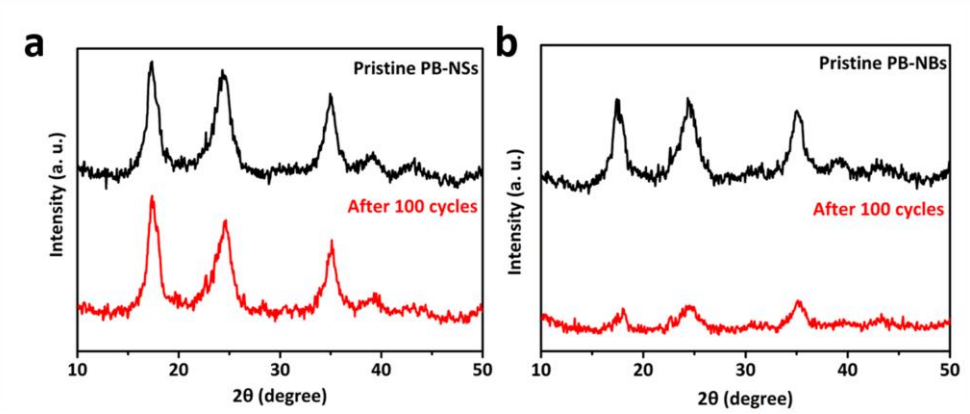

Fig S13. XRD patterns of pristine and cycled electrode materials for (a) PB-NSs and (b) PB-NBs.

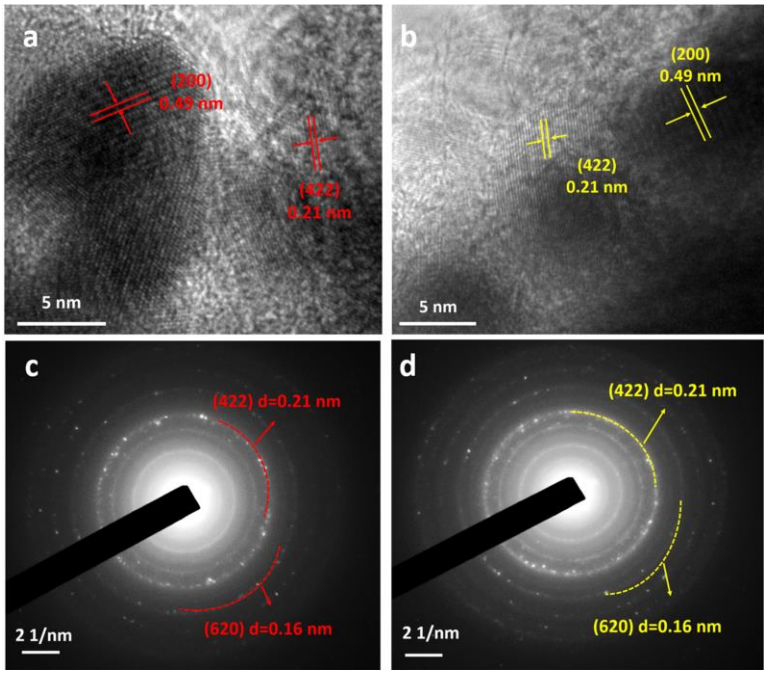

Fig S14. The (a) HRTEM image and (c) SAED pattern of pristine PB-NSs. (b) HRTEM image and (d) SAED pattern of PB-NSs after 20 cycles at 50 mA g^{-1}.

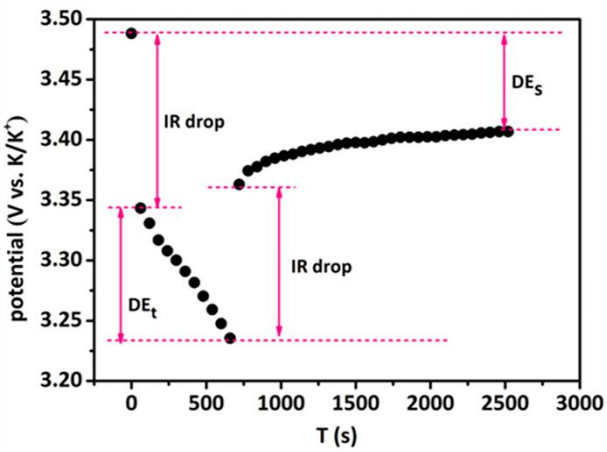

Fig S15. The regional GITT potential response curves with time.

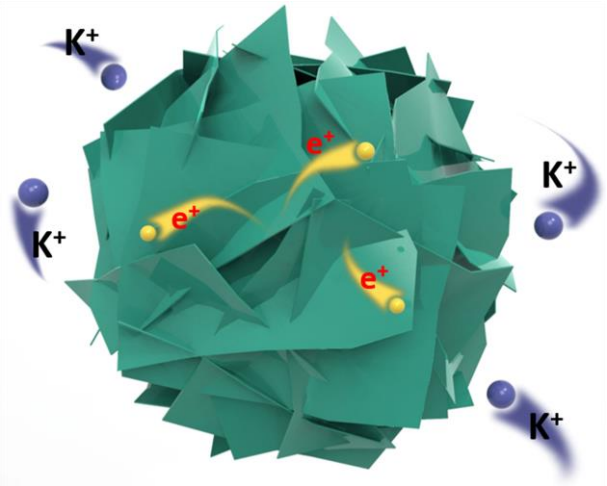

Fig S16. The schematic of ions and charge transport process.

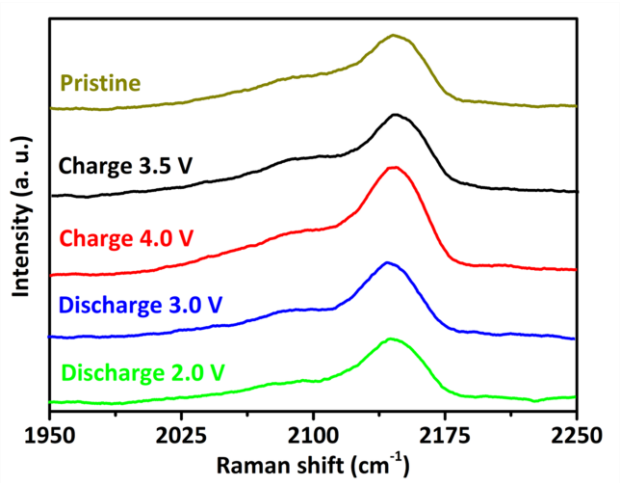

Fig S17. Raman spectra collected at different charge and discharge states for PB-NSs at 50 mA g^{-1}.

Table S1. ICP results of the PB-NSs and PB-NBs

Sample	Element	Weight%	Atomic%
PB-NSs	K	0.08	0.205
	Fe	0.64	1.143
PB-NBs	K	0.07	0.179
	Fe	0.71	1.37